Reciprocal interaction between I_{K1} and I_f in biological pacemakers: A simulation study

Running Title: Role of I_{K1} and I_f in bio-pacemaking

Yacong Li[1,2], Kuanquan Wang[1], Qince Li[2,3], Jules C. Hancox[4], Henggui Zhang[2,3,5]*

[1] School of Computer Science and Technology, Harbin Institute of Technology, Harbin, Heilongjiang Province, China

[2] Biological Physics Group, School of Physics and astronomy, The University of Manchester, Manchester, the Great Manchester, UK

[3] Peng Cheng Laboratory, Shenzhen, Guangdong Province, China

[4] School of Physiology, Pharmacology and Neuroscience, Medical Sciences Building, University Walk, Bristol, UK

[5] Key Laboratory of Medical Electrophysiology of Ministry of Education and Medical Electrophysiological Key Laboratory of Sichuan Province, Institute of Cardiovascular Research, Southwest Medical University, Luzhou, Sichuan Province, China

* **Correspondence**: Henggui Zhang; henggui.zhang@manchester.ac.uk

Abstract

Pacemaking dysfunction (PD) may result in heart rhythm disorders, syncope or even death. Current treatment of PD using implanted electronic pacemaker has some limitations, such as finite battery life and the risk of repeated surgery. As such, the biological pacemaker has been proposed as a potential alternative to the electronic pacemaker for PD treatment. Experimentally it has been shown that bio-engineered pacemaker cells can be generated from non-rhythmic ventricular myocytes (VMs) by knocking down genes related to the inward rectifier potassium channel current (I_{K1}) or by overexpressing hyperpolarization-activated cyclic nucleotide gated channel genes responsible for the "funny" current (I_f). Such approaches can turn the VM cells into rhythmic pacemaker cells. However, it is unclear if a bio-engineered pacemaker based on the modification of I_{K1}- and I_f-related channels simultaneously would enhance the ability and stability of bio-engineered pacemaking action potentials (APs). This study aimed to investigate by a computational approach the combined effects of modifying I_{K1} and I_f density on the initiation of pacemaking activity in human ventricular cell models. First, the possible mechanism(s) responsible for VMs to generate spontaneous pacemaking APs by changing the density of I_{K1} and I_f were investigated. Then the integral action of targeting both I_{K1} and I_f simultaneously on the pacemaking APs was analysed. Our results showed a reciprocal interaction between I_{K1} and I_f on generating stable and robust pacemaking APs in VMs. In addition, we thoroughly investigated the dynamical behaviours of automatic rhythms in VMs in the I_{K1} and I_f parameter space, providing optimal parameter ranges for a robust pacemaker cell. In conclusion, to the best of our knowledge, this study provides a novel theoretical basis for generating stable and robust pacemaker cells from non-pacemaking VMs, which may be helpful in designing engineered biological pacemakers for application purposes.

Keywords: bio-pacemaker, sinoatrial node, funny current (I_f), inward rectifier potassium channel current (I_{K1}), reciprocal interaction, stable pacemaking

Author Summary

Pacemaking dysfunction has become one of the most serious cardiac diseases, which may result in arrhythmia and even death. The treatment of pacemaking dysfunction by electronic pacemaker has saved millions of people in the past fifty years. But not every patient can benefit from it because of possible limitations, such as surgical implication and lack of response to autonomic stimulus. The development of bio-pacemaker based on gene engineering technology provides a promising alternative to electronic pacemaker by manipulating the gene expression of cardiac cells. However, it is still unclear how a stable and robust bio-pacemaker can be generated. The present study aims to elucidate possible mechanisms responsible for a bio-engineered pacemaker by using a computational electrophysiological model of pacemaking cells based on modifying ion channel properties of I_{K1} and incorporating I_f in a human ventricular cell model, mimicking experimental approaches of gene engineering. Using the model, possible pacemaking mechanisms in non-pacemaking cells, as well as factors responsible for generating robust and stable biological pacemaker, were investigated. It was shown that the reciprocal interaction between reduction of I_{K1} and incorporation of I_f played an important role for producing robust and stable pacemaking. This study provides a novel insight into understanding of the initiation of pacemaking behaviours in non-rhythmic cardiac myocytes, providing a theoretical basis for experimental designing of biological pacemakers.

Introduction

Currently, the electronic pacemaker implantation is the only non-pharmacological therapy for some patients with pacemaking dysfunctions (PD), such as sick sinus syndrome and atrioventricular heart-block, but it has some possible limitations (1). Implantation of pacemaker device may have complications for patients, especially for aged ones because of their infirm health (2). Pediatric patients can receive electronic pacemakers; however, the device has to be replaced as they grow and repeated surgeries are needed (3). Electronic devices can be subject to electromagnetic interference (4), which causes inconvenience to the patients. A further issue is that classical electronic pacemakers are insensitive not only to hormone stimulation (5) but also to autonomic

emotion responsiveness (4), although there are some attempts to make them respond to autonomic nervous control (6). In addition, the long-term use of electronic pacemakers has been reported to increase the risk of heart failure (7). Appropriately designed biological pacemakers (bio-pacemakers) have the potential to overcome some of the limitations of electrical device use (8). For example, engineered bio-pacemakers could potentially involve only minor surgical trauma for implantation as well as opportune chronotropic responses to creature emotion (9). In previous experimental studies, it has been shown that a bio-pacemaker can be engineered *via* adenoviral gene transduction (10-12) or lentiviral vector (13, 14) techniques, by which non-pacemaking cardiac myocytes (CMs) can be transformed to rhythmic pacemaker-like cells.

The native cardiac primary pacemaker, sinoatrial node (SAN), is a special region comprised of cells with distinct electrophysiological properties to cells in the working myocardium. Such intrinsic and special electrophysiological properties of SAN cells are mainly manifested by their small if not absent inward rectifier potassium channel current (I_{K1}) (15), but a large "funny" current (I_f) (16) that is almost absent in atrial and ventricular cells. In addition to absence of I_{K1} and presence of I_f, T-type Ca^{2+} channel current (I_{CaT}) (17) and sustained inward current (I_{st}) (18) also contribute to spontaneous pacemaking activity in SAN cells. Such unique electrophysiological properties of SAN cells form a theoretical basis to engineer non-pacemaking CMs into spontaneous pacemaker cells. These non-pacemaker cells include native CMs, such as ventricular (11, 19-21), atrial (22) or bundle branch myocytes (23). They can also be stem cells, such as embryonic stem cells (24-26), bone marrow stem cells (13, 27, 28), adipose-derived stem cells (29-31), or induced pluripotent stem cell (14, 32, 33).

With gene therapy, these cells are manipulated to provoke automaticity. In previous studies, knocking off the *Kir2.1* gene to reduce the expression of I_{K1} promoted spontaneous rhythms in newborn murine ventricular myocytes (VMs) (19); by reprogramming the *Kir2.1* gene in guinea-pigs, VMs also produced pacemaker activity when I_{K1} was suppressed by more than 80% (11, 20). As I_f plays an important role in the native SAN cell pacemaking, a parallel gene therapy manipulation to create engineered bio-pacemaker has been carried out by expressing the *HCN* gene family in non-rhythmic cardiac myocytes (34). It has

been shown that expressing *HCN2* produced escape beats in canine CMs (22, 23) and initiated spontaneous beats in neonatal rat VMs (21). *HCN* expression in stem cells-induced-CMs also enhanced their pacemaking rate (13, 27, 28, 35, 36). Overexpressing *HCN4* can also induce spontaneous pacemaking activity in mouse embryonic stem cells (37). However, acute expression of the *HCN* gene might have a side effect on the normal cardiac pacemaking activity (38-40) and the overexpression of the *HCN* gene in VMs can cause ectopic pacemaker automaticity and even arrhythmicity (41).

It has been suggested that a combined manipulation of I_{K1} and I_f may be a better alternative for creating a bio-pacemaker (42). It has been demonstrated that the expression of transcriptional regulator *TBX18*, which influenced both I_f and I_{K1} expression, generated appropriate autonomic responses in non-pacemaking CMs (10, 31, 43). In addition, reprogramming *TBX18* in porcine VMs did not show the increase of arrhythmia risk (12), indicating the probable superiority of manipulating I_{K1} and I_f jointly for generating a bio-pacemaker. Furthermore, Chen et al. (44) attempted to explore the generation of oscillation by manipulating the expressing level of *Kir2.1* and the *HCN* genes and suggested that a dynamic balance between *Kir2.1* and *HCN* was essential to initiate oscillation in HEK293 cells. In the absence of I_{K1}, spontaneous rhythmic oscillations might be inhibited due to an insufficiently repolarized membrane potential to activate I_f. However, HEK293 cells lack all the other ionic channels present in native SAN myocytes.

Computational modelling offers a means to investigate different approaches to generating stable pacemaking activity. It has been used to study possible roles of down-regulating I_{K1} in VMs (45-47) and combined action of overexpression of I_f with down-regulation of I_{K1} in inducing spontaneous pacemaking activity in SAN (42). Bifurcation analysis has also been used to explore the effect of changes in some individual ion channel current on the pacemaking activities of SAN cells (48) and genesis of automaticity in VMs (46, 49), showing the role of I_{K1}, I_f, I_{st} and Na^+/Ca^{2+} exchange current (I_{NaCa}) in modulating the initiation and stability of pacemaking activity (49). But this approach was applied to simplified CMs model (46) and interplay between more than one ion channel currents on modulating bio-pacemaker APs has not been comprehensively investigated yet.

In this study, we constructed a bio-pacemaker model based on a human non-rhythmic VMs model (50) by manipulating I_{K1} and incorporating I_f (51) into the model. The aim of this study was to investigate (i) possible mechanism(s) underlying the pacemaking activity of the VMs in the I_{K1} and I_f parameter space; and (ii) the reciprocal interaction of reduced I_{K1} and increased I_f in generating stable pacemaking action potentials (APs) in them. In addition, possible factors responsible for impaired pacemaking activity due to inappropriate ratio between I_{K1} and I_f were also investigated. This study provides insightful understandings to generating stable and robust engineered bio-pacemaker.

Results

Initiation of transient spontaneous depolarization

In the basal VM cell model with the suppression of I_{K1} by 70% (the density of I_{K1} at -80 mV was 0.297 pA/pF), incorporating of I_f (with a current density of -0.63 pA/pF at -80 mV in the I-V curve of I_f (S1B Fig)) was unable to depolarize the membrane potential and lead to spontaneous pacemaking activity because the excessive outward current of I_{K1} counteracted the inward depolarizing current. This state can be described by State-1 as shown in Eq. 8. However, when the density of I_f was increased to -1.89 pA/pF, spontaneous depolarization was provoked at the beginning of the transition period, however, the automaticity self-terminated after 1.63×10^5 ms (Fig 1 A), showing a State-2 behaviour as described in Eq. 9.

We analysed possible ion channel mechanisms responsible for unstable and self-terminating pacemaking APs with the current densities of (I_{K1}, I_f) at (0.297pA/pF, -1.89 pA/pF) ('CASE 1'). Results in Fig 1 showed that during the time course of the spontaneous pacemaking, there were changes of intracellular ionic concentrations and the MDP. Through the Na^+ permeability of I_f, there was extra Na^+ flowing into the cytoplasm during each of the APs, leading the intracellular Na^+ concentration ($[Na^+]_i$) to increase from 7.67 to 11.8 mM (Fig 1 B). The increased $[Na^+]_i$ augmented the feedback mechanism of Na^+/K^+ pumping activity, by which the Na^+/K^+ pump current (I_{NaK}) increased gradually with time (Fig 1 E). In addition, there was also an accumulation of the intracellular Ca^{2+} concentration ($[Ca^{2+}]_i$, Fig 1 C) during the time course of spontaneous pacemaking APs. Such an

accumulation of $[Ca^{2+}]_i$ was due to the fact that the automaticity in VMs shortened the DI between two successive APs, leaving insufficient time for Ca^{2+} in the cytoplasm to be extruded to restore to its initial value after each cycle of excitation. This consequentially led to overload in $[Ca^{2+}]_i$, which suppressed the extent of the activation degree of the L-type calcium current (I_{CaL}, Fig 1 F), especially during the phase 0 of the pacemaking action potential. Furthermore, the overloaded $[Ca^{2+}]_i$ increased the I_{NaCa} (S2 Fig) gradually with time, resulting in an elevated MDP (Fig 1 H) that inhibited the activation degree of the fast sodium channel current (I_{Na}, Fig 1 D). All of these factors worked together, inhibiting the membrane potential to reach the take-off potential, leading to self-terminated automaticity at 1.63×10^5 ms (Fig 1 G).

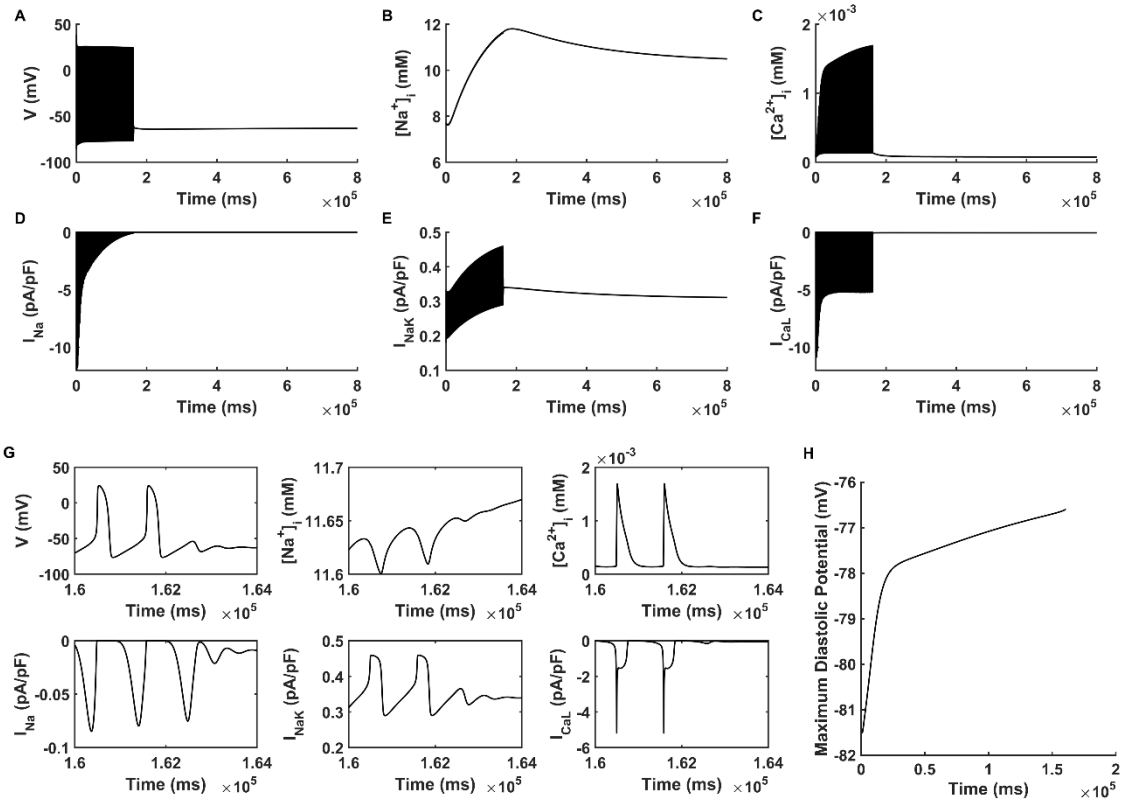

Fig 1. Transient spontaneous pacemaking behaviour.

(A-F) Membrane potential (V), intracellular Na^+ concentration ($[Na^+]_i$), intracellular Ca^{2+} concentration ($[Ca^{2+}]_i$), fast sodium current (I_{Na}), L-type calcium channel current (I_{CaL}) and Na^+/K^+ pumping current (I_{NaK}) with the current densities of (I_{K1}, I_f) at (0.297pA/pF, -1.89 pA/pF) during the entire simulating period of 800 s. (G) Expanded plots of (A-F) for the time course of

pacemaking self-termination (1.6×10^5 ms to 1.64×10^5 ms). H: Maximum diastolic potential of spontaneous pacemaking behaviour of (A).

It was also possible to generate automaticity in the model by fixing the current density of I_f at a low value, but with a further reduction in I_{K1} density. S3 Fig shows the results when I_f was held at -0.63 pA/pF, the current density of I_{K1} was reduced to 0.178 pA/pF. In this case, pacemaking activity appeared in the model, but the automaticity was unstable and self-terminated due to similar mechanisms as shown in Fig1 for the increased-I_f situation.

Bursting pacemaking behaviour

Fig 2 shows the intermittent bursting behaviour, which is generated with a different combination of I_{K1} and I_f current densities in the model. In the figure, the current densities of (I_{K1}, I_f) were held at (0.297 pA/pF, -2.52 pA/pF) (defined as 'CASE 2'). Such kind of pacemaking state can be classified as State-3 (Eq. 10).

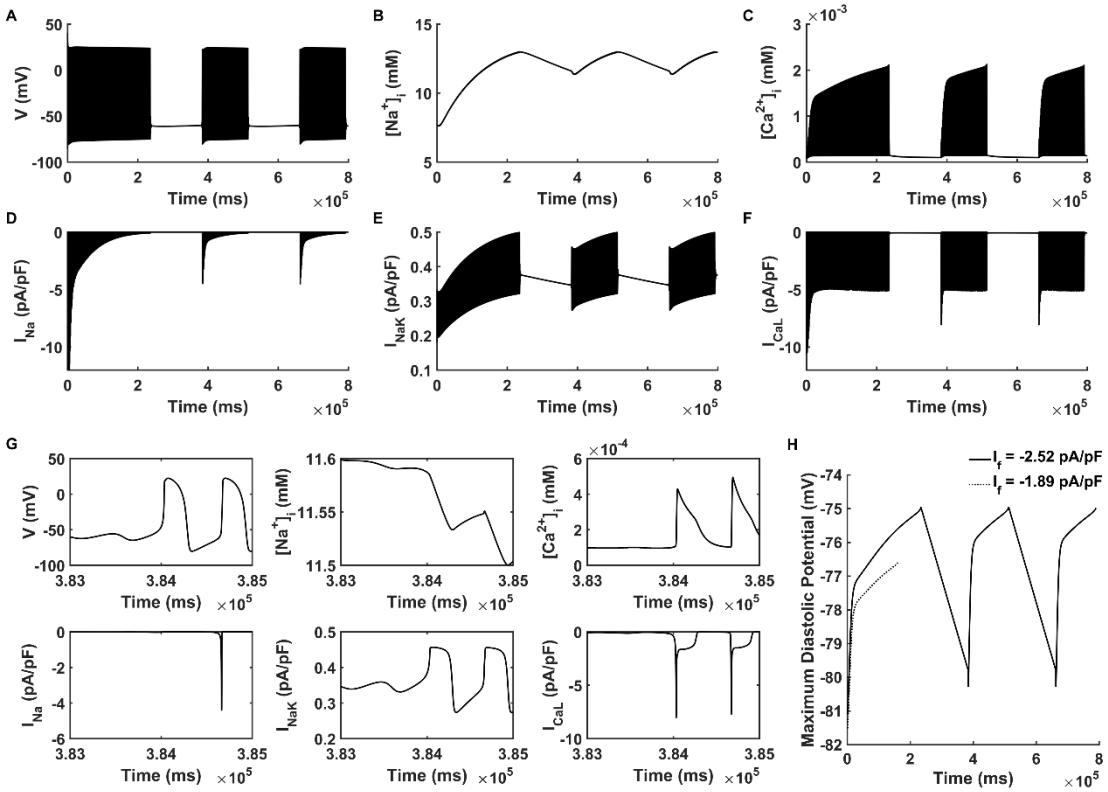

Fig 2. Bursting pacemaking behaviour.

(A-F) Membrane potential (V), intracellular Na^+ concentration ($[Na^+]_i$), intracellular Ca^{2+} concentration ($[Ca^{2+}]_i$), fast sodium channel current (I_{Na}), Na^+/K^+ pumping current (I_{NaK}) and L-type calcium channel current (I_{CaL}) with the current densities of (I_{K1}, I_f) at (0.297 pA/pF, -2.52 pA/pF) during the entire simulating period of 800 s. (G) Expanded plots of (A-F) for the time course of pacemaking resumption (3.83×10^5 ms to 3.85×10^5 ms). H: Maximum diastolic potential of automatic pacemaking activity when I_f is -2.52 and -1.89 pA/pF (solid and dotted line respectively).

In CASE 2, the spontaneous oscillation was unstable, characterized by self-termination and then resumption after a quiescent period (Fig 2 A). Similar to CASE 1, the self-termination was accompanied by the overload of $[Na^+]_i$ (Fig 2 B), the accumulation of $[Ca^{2+}]_i$ (Fig 2 C), which caused the reduction of I_{Na} (Fig 2 D), the increase of I_{NaK} (Fig 2 E) and the decrease of I_{CaL} (Fig 2 G). This suggested that the underlying mechanisms responsible for the self-termination of the pacemaking APs were similar to those of CASE 1.

It is of interest to analyse the mechanism(s) for the resumption of the pacemaking APs after a long pause. It was shown that, during the time course of the quiescent interval (from 2.36×10^5 ms to 3.84×10^5 ms in Fig 2 A-F), the intracellular Na^+ (Fig 2 B) continued to be extruded out of the cell by I_{NaK} (Fig 2 E), and the intracellular Ca^{2+} (Fig 2 C) extruded by the I_{NaCa} (S4A Fig). As such, the $[Na^+]_i$ (Fig 2 B) and $[Ca^{2+}]_i$ (Fig 2 C) gradually decreased over time. A decrease in $[Na^+]_i$ led to a gradually reduced I_{NaK} over the time course of quiescence (Fig 2 E), which decreased its suppressive effect on depolarization. During the time period of quiescence, I_{CaL} kept at a small magnitude (Fig 2 F). *Via* I_{NaCa} (S4 Fig), the intracellular Ca^{2+} was kept to be extruded out of the cell, leading to a decreased $[Ca^{2+}]_i$. Consequentially, a decrease in $[Ca^{2+}]_i$ resulted in a reduced calcium-dependent inactivation of I_{CaL}, leading to an increased I_{CaL} (Fig 2 G), which facilitated the action potential generation. Moreover, as compared with CASE 1, the increase in I_f also helped to produce a more depolarized MDP (Fig 2 H), allowing the membrane potential more easily to reach the take-off potential for initiation of the upstroke. All of these actions worked in combination to produce a full course of action potential with a sufficient amplitude that activated sufficient outward currents to repolarize the cell membrane to a range that

activated I_f and I_{Na}, facilitating the resumption of the spontaneous pacemaking activity at 3.847×10^5 ms (Fig 2 G). This process of self-termination and resumption repeated alternately, which constituted bursting behaviour.

Persistent pacemaking activity

A further increase in I_f ((I_{K1}, I_f) at (0.297 pA/pF, -3.15 pA/pF)) produced a series of persistent spontaneous APs. Results are shown in Fig 3 (grey lines) for APs (Fig 3 A), together with a phase portrait of membrane potential (V) and total membrane channel current (I_{total}) (Fig 3 B), I_{K1} (Fig 3 C), and I_{CaL} (Fig 3 D). Although the spontaneous APs were sustained during the entire simulation period of 800 s, there were some incomplete depolarizations observed periodically (Fig 3 A, grey line) which can be classified as State-4 according to Eq. 11. This pacemaking situation was termed as 'CASE 3'.

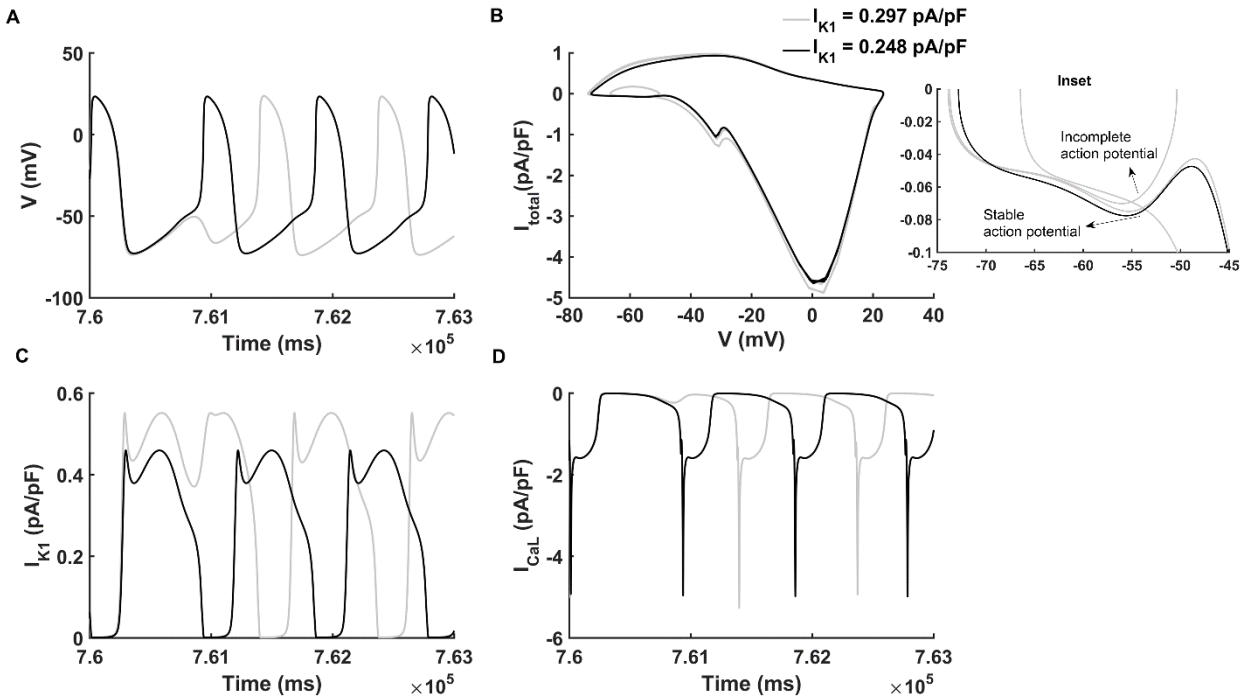

Fig 3. Persistent pacemaking activity.

The current densities of (I_{K1}, I_f) of stable pacemaking activity and periodically incomplete pacemaking activity are at (0.248 pA/pF, -3.15 pA/pF) (black lines) and (0.297 pA/pF, -3.15 pA/pF) (grey lines) respectively. (A-D) The membrane potential (V), phase portraits of membrane potential against the total membrane channel current (I_{total}), inward rectifier potassium channel

current (I_{K1}) and L-type calcium channel current (I_{CaL}) with simulating time course from 7.6×10^5 to 7.63×10^5 ms. (Inset) Expanded plot for phase diagram during V from -75 to -45 mV and I_{total} from -0.1 to 0 pA/pF.

When the density of I_{K1} was further reduced to 0.248 pA/pF (Fig 3 C, black line), a stable pacemaking activity was established (Fig 3A, black line), with an average CL of 895 ms and MDP of -72.63 mV. This kind of pacemaking state can be described as State-5 by Eq. 12. In this condition, the pacemaking activity was robust and the pacing CL was close to that of the native human SAN cells (approximately 800 - 1000 ms (52)). We termed stable pacemaking activity with (I_{K1}, I_f) at (0.248 pA/pF, -3.15 pA/pF) as 'CASE 4'.

In order to understand potential mechanism(s) underlying the genesis of incomplete pacemaking potentials in CASE 3, phase portraits of membrane potential against I_{total} for incomplete (grey line) and complete (black line) depolarization APs were plotted and superimposed for comparison, as shown in Fig 3 B, with a highlight of phase portraits during the diastolic pacemaking potential range from -75 mV to about -45 mV being shown in the inset. In the case of incomplete depolarization (CASE 3), there was a greater I_{K1} (Fig 3 C) that counteracted the inward depolarizing current, leading to a smaller I_{total} during the diastolic depolarization phase (see the grey line in Fig 3 B and the inset). Consequentially the membrane potential failed to reach the take-off potential for the activation of I_{CaL} (Fig 3 D, grey line), leading to an incomplete course of action potential (Fig 3 A, grey line). In CASE 4, with a reduced I_{K1} (Fig 3 C, black line), there was a greater I_{total} during the diastolic depolarization phase (Fig 3 B and the inset, black line), which drove the membrane potential to reach the take-off potential for the activation of I_{CaL} (Fig 3 D, black line), leading to the upstroke of the action potential.

The frequency for the appearance of the incomplete AP was dependent on the density of I_{K1}. Incomplete depolarization occurred less frequently, with progressively smaller I_{K1}. By way of illustration, the incomplete depolarization appeared once every three cycles with the I_{K1} density at 0.297 pA/pF in CASE 3 (S5A Fig), but this became once every five cycles when I_{K1} density was reduced to 0. 277 pA/pF I_{K1} (S5B Fig). This suggested that a large residual of I_{K1} in the VM model might result in the failure of

complete depolarization.

Dynamic analysis in I_{K1} and I_f parameter space

Dynamic pacemaker AP behaviours were dependent on the balance of I_{K1} and I_f interactions. Further simulations were conducted in the I_{K1} and I_f parameter space to characterize this dependence. Results are shown in Fig 4. With differing combinations of I_{K1} and I_f density, five different regions for distinctive pacemaking dynamics could be discerned, including stable pacemaking activity (blue area, features described by Eq. 12), intermittence of failed depolarization (yellow area, features described by Eq. 11), bursting pacemaking behaviour (orange area, features described by Eq. 10), transient pacemaking activity (green area, features described by Eq. 9), and no automaticity (grey area, features described by Eq. 8). In each category, representative membrane potentials are illustrated at the bottom panel of the Fig 4.

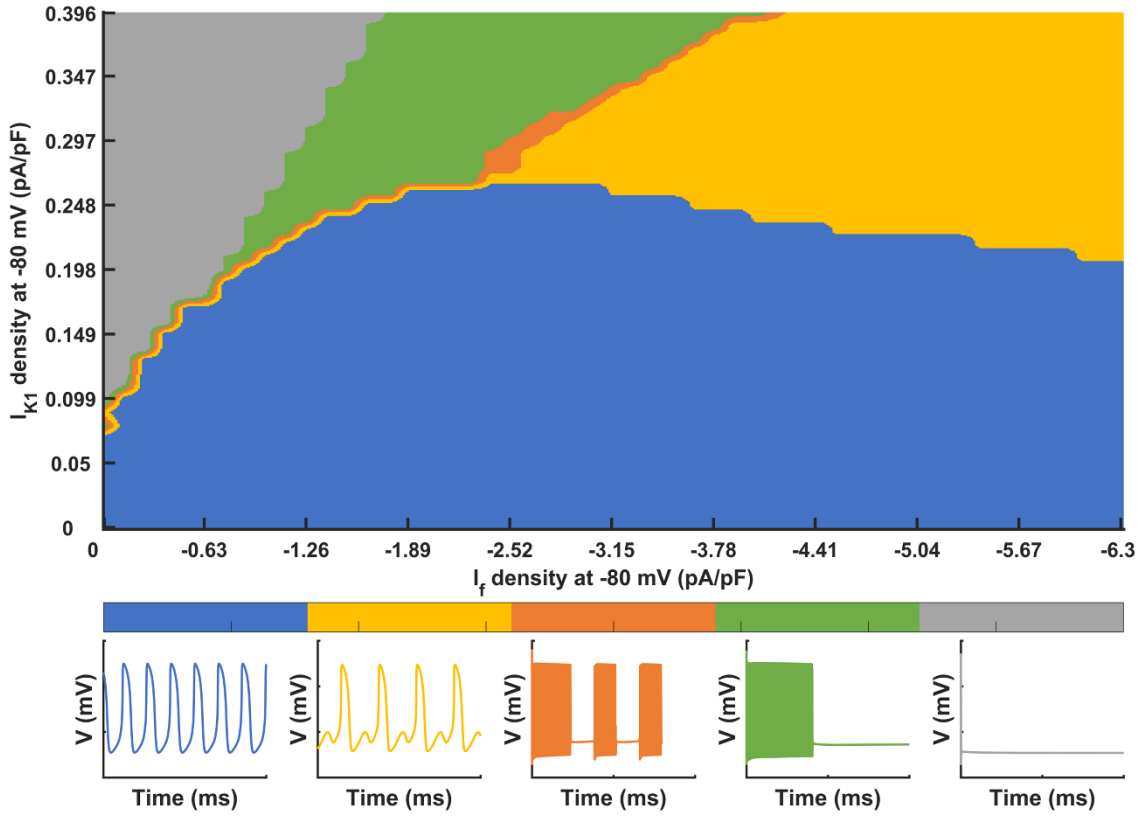

Fig 4. The dynamical behaviours of the pacemaking action potentials in I_{K1} and I_f parameter space.

Blue: stable pacemaking activity; Yellow: persistent pacemaking activity with periodic incomplete depolarization. Orange:

bursting pacemaking behaviour. Green: transient spontaneous pacemaking behaviour. Gray: no spontaneous pacemaking behaviour. In each category, the typical pacemaking action potentials are illustrated at the bottom panel.

With a fixed I_f density, alterations to I_{K1} could produce different types of pacemaking activities and this also applied when I_{K1} was fixed whilst I_f was changed. To illustrate, when I_f density was fixed at a density between -0.63 and -2.52 pA/pF, with a 60 – 80% block of I_{K1} (i.e., I_{K1} density at -80 mV was in the range of 0.198-0.396 pA/pF), pacemaking activity was generated but with self-termination (Fig 4, green area). Then, a further reduction in I_{K1} or a slight increase in I_f induced bursting pacemaking behaviour, as shown by the orange area in Fig 4, which was between the boundaries marking the persistent automaticity and transient pacemaking activity regions. A further increase in I_f or suppression in I_{K1} could produce persistent automaticity (Fig 4, yellow and blue area). But when I_{K1} was greater than about 0.248 pA/pF, incomplete depolarization appeared periodically (Fig 4, yellow area). Finally, a stable and spontaneous pacemaking activity could be generated when I_{K1} was decreased to less than 0.248 pA/pF at -80 mV with I_f included (Fig 4, blue area).

Reciprocal role of I_f and I_{K1} in generating pacemaking APs

Further analysis was conducted to investigate the reciprocal role of reduced I_{K1} and increased I_f in generating pacemaking APs. By sufficiently reducing I_{K1} to a density of 0.05 pA/pF alone, the model was able to generate spontaneous APs with a CL of 1011 ms. In this case, the incorporation of I_f with a small density helped to boost the pacemaking activity and increase the pacemaking frequency. It was shown that with the incorporation of I_f at a density of 0.63 pA/pF, the CL was reduced by 233 ms, changing from 1011 ms to 778 ms (Fig 5 A). Compared with the case of I_f absence, incorporation of I_f - even with a small density (-0.63 pA/pF) - helped to depolarize cell membrane potential during the early DI phase (Fig 5 A and C). Moreover, the incorporation of I_f led to an accumulation of $[Na^+]_i$ (Fig 5 B) then increased amplitude of I_{NaCa} (Fig 5 D), which also contributed to the depolarization of membrane potential. As a result, the incorporation of I_f facilitated genesis of spontaneous APs and shortened the DI significantly, thus decreased the CL.

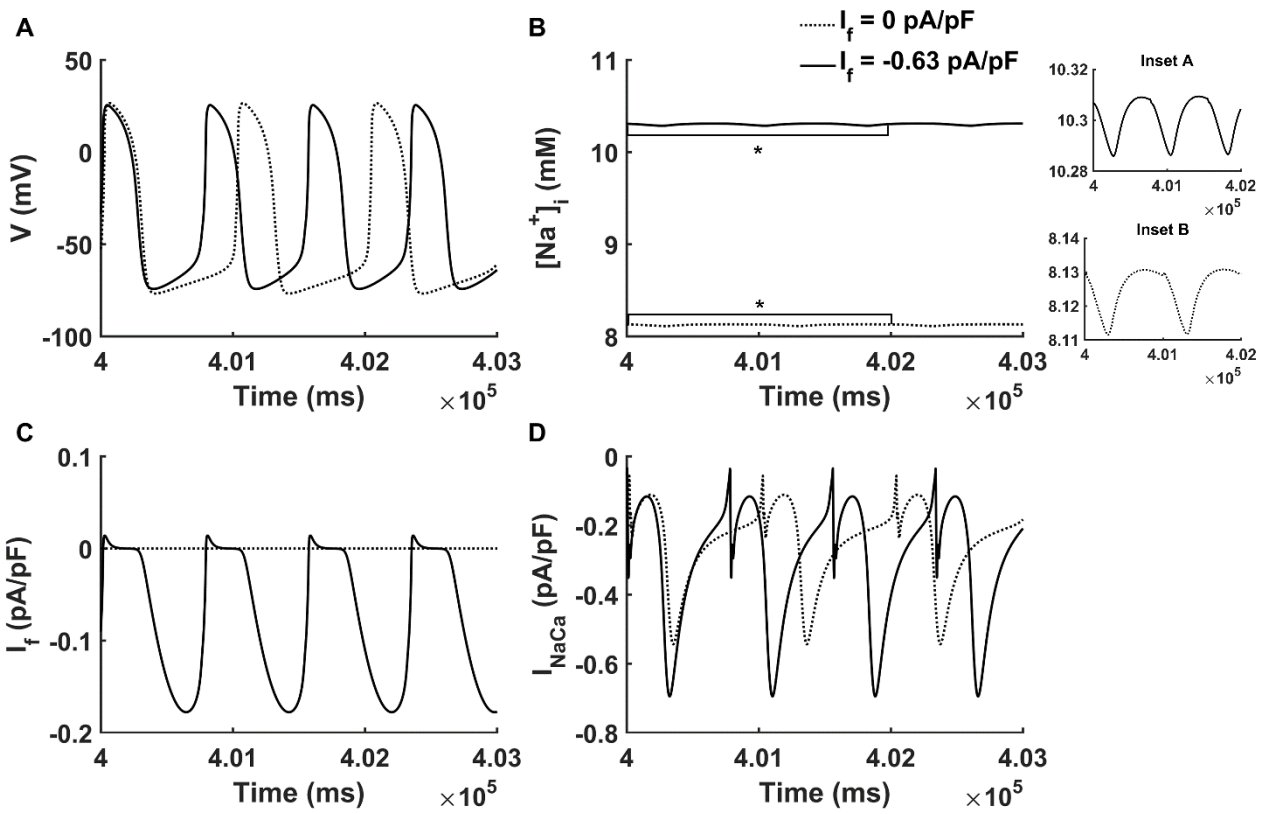

Fig 5. Role of I_f in pacemaking ability.

(A-D) The membrane potential (V), intracellular Na^+ concentration ($[Na^+]_i$), hyperpolarization-activated channel current (I_f), Na^+/Ca^{2+} exchange current (I_{NaCa}) with simulating time course from 4×10^5 to 4.03×10^5 ms when the current densities of (I_{K1}, I_f) are at (0.05 pA/pF, 0 pA/pF) and (0.05 pA/pF, -0.63 pA/pF) (dotted and solid line respectively). (Inset A-B) Expanded plots of $[Na^+]_i$ traces for the time course marked by the horizontal brackets with asterisks in (B).

With a fixed I_{K1} density of 0.05 pA/pF, the relationship between the computed CL of pacemaking APs and I_f density was found to be nonlinear as shown in Figure 6 A. In a range from -0.126 to -2.52 pA/pF, an increase in I_f density produced a marked decrease in the CL (Fig 6 A), which was associated with an increase in the rate of membrane depolarization during the DI (diastolic depolarizing rate) (S6B Fig). In this range, an increase in I_f caused an elevated MDP (Fig 6 B), as well as an accumulation of $[Na^+]_i$ (Fig 6 C), which enhanced I_{NaCa} (Fig 6 D). All of these contributed to the acceleration of the pacemaking activity. However, when I_f density was over -2.52 pA/pF, there was a less dramatic decrease in CL with an increase of I_f (Fig 6 A). This was

attributable to a reduced I_{Na} (Fig 6 F) as a consequence of gradual elevation of the MDP (Fig 6 B). Another factor was that the maximum density of I_f was not increased linearly (Fig 6 E) because of elevated MDP.

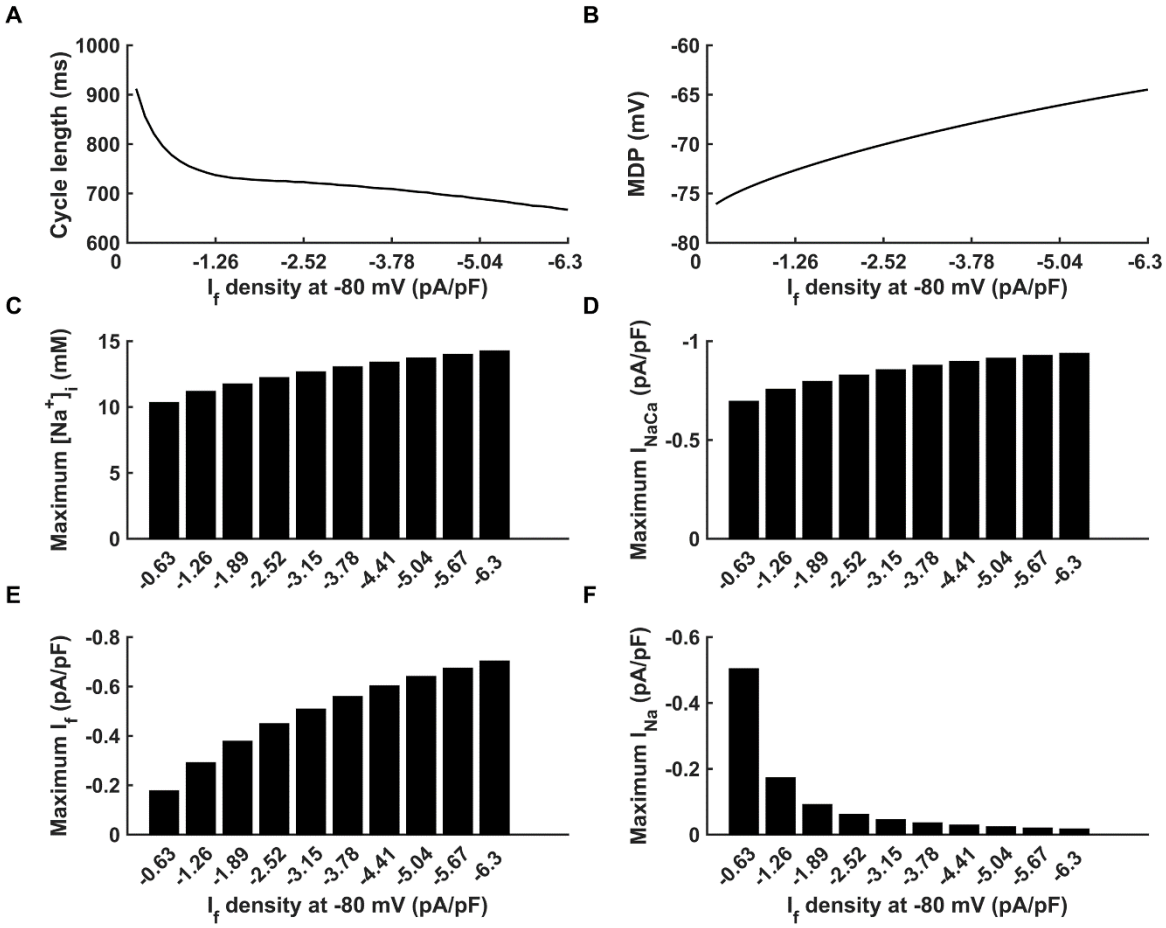

Fig 6. Effect of I_f density on the pacemaking cycle length under fixed I_{K1} density.

I_{K1} density is fixed at 0.05 pA/pF. (A-B) Change of cycle length and maximum diastolic potential (MDP) with the increase of I_f from 0 to -6.3 pA/pF. (C-F) Change of maximum intracellular Na^+ concentration ($[Na^+]_i$), maximum Na^+/Ca^{2+} exchange current (INaCa), maximum funny current (I_f) and maximum fast sodium current (I_{Na}) during a pacemaking period with the increase of I_f.

Depending on the I_{K1} density, the relationship between CL and I_f density could also be biphasic as shown in Fig 7. With a small I_{K1} density (0.05 pA/pF), the measured CL decreased monotonically with the increase in I_f density (Fig 7 A, dotted line). However, with a large I_{K1} (0.198 pA/pF), the measured CL first decreased with an increased I_f density, but then increased with it

when I_f density was greater than -3.15 pA/pF, implicating a slowdown in the pacemaking activity with the increase of I_f (Fig 7 A, solid line). Such a slowdown of pacemaking APs with an increased I_f was mainly due to the prolonged DI (S7 Fig). This was attributable to the delicate balance between the total integral of three dominant inward currents (I_{Na}, I_{NaCa} and I_f) (I_{in} as defined in Eq. 14) and the total integral of four dominant outward currents (I_{K1}, I_{NaK}, I_{Kr} and I_{Ks}) (I_{out} as defined in Eq. 15) during the DI phase (Fig 7 B and C). At a low I_{K1} density of 0.05 pA/pF, with the increase in I_f density, there was a monotonic increase in both of I_{in} and I_{out}, and the balance of them resulted in a monotonic decrease of CL (Fig 7, dotted lines). However, at a large I_{K1} density (e.g. 0.198 pA/pF), an increase of I_f was associated with a monotonic increase in I_{out} (Fig 7 C, black line), but had a different impact on I_{in}, which reached at a flat magnitude after I_f density was greater than -3.15 pA/pF (Fig 7 B, black line). Consequentially, at large I_f, a greater I_{out} out balanced the I_{in}, leading to a prolonged DI that increased the CL.

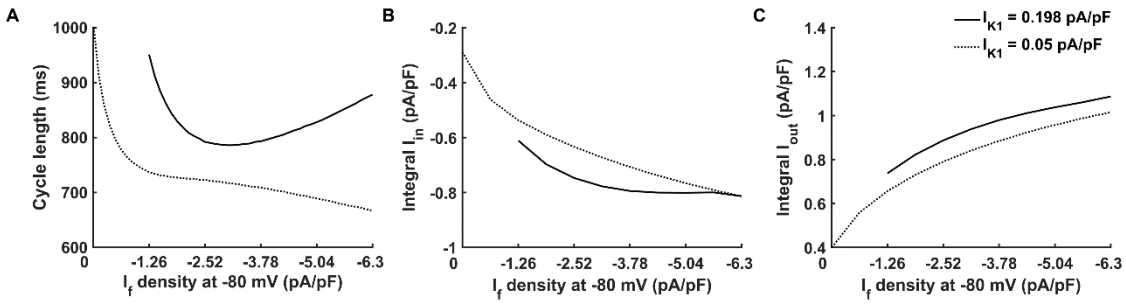

Fig 7. Effect of I_f density on the pacemaking cycle length under different I_{K1} density.

I_{K1} density is 0.198 (solid line) and 0.05 pA/pF (dotted line) at -80 mV. (A) Change of cycle length with the increase of I_f from 0 to -6.3 pA/pF. (B) Change of the total integral of main inward currents (Integral I_{in}) during diastolic interval phase. The inward currents include fast sodium current (I_{Na}), Na^+/Ca^{2+} exchange current (I_{NaCa}) and funny current (I_f). (C) Change of the total integral of main outward currents (Integral I_{out}) during diastolic interval phase. The outward currents include inward rectifier potassium channel current (I_{K1}), Na^+/K^+ pumping current (I_{NaK}), rapid delayed rectifier potassium channel current (I_{Kr}) and slow delayed rectifier potassium channel current (I_{Ks}).

Pacemaking cycle length in I_{K1} and I_f parameter space

A systematic analysis of the relationship between the calculated CL in the I_{K1} and I_f density parameter space is presented in Fig 8. In the figure, the measured CL was coloured from 650 ms in dark red to 1000 ms in yellow. In this study, we regarded persistent pacemaking action potential with CL 1000 ms or less as 'valid pacemaking activity', therefore, only the CLs of the valid pacemaking potentials are shown in Fig 8.

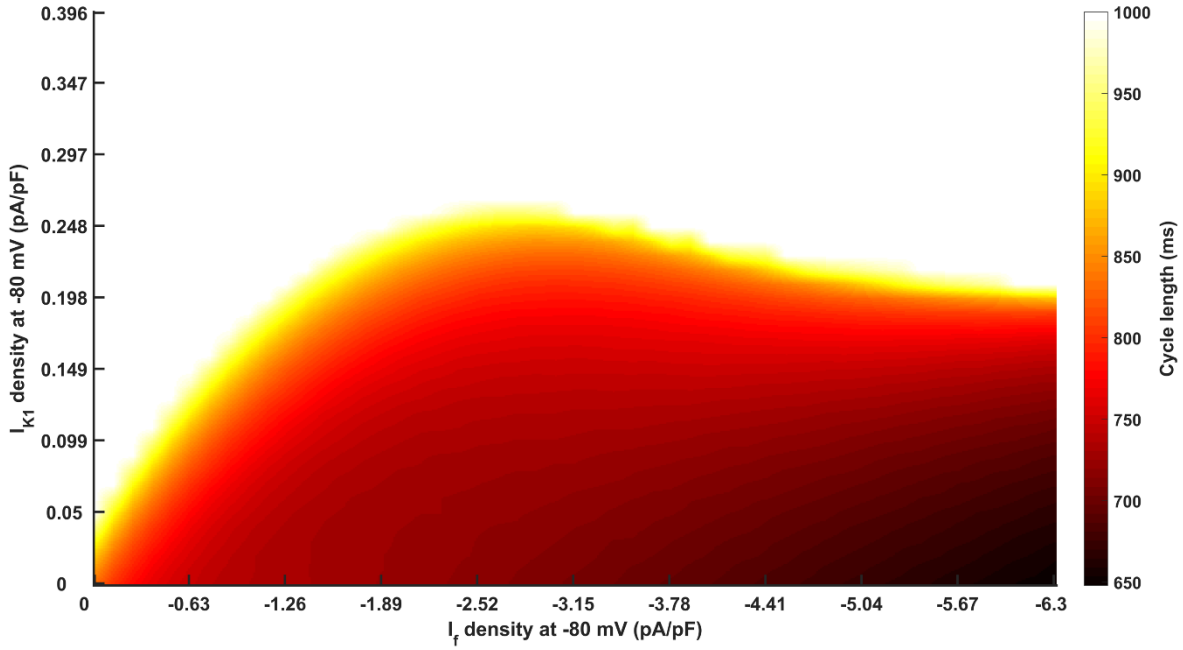

Fig 8. Measured cycle length in the I_{K1} and I_f density parameter space.

The density of I_{K1} is from 0 to 0.396 pA/pF and the density of I_f is from 0 to -6.3 pA/pF at -80 mV. The measured CL is coloured from 650 ms in dark red to 1000 ms in yellow. White means that pacemaking cycle length is 'invalid' (more than 1000 ms) or membrane potential is not persistent during the whole simulating time course.

It was shown that a sufficient depression in I_{K1} (up to 75%; I_{K1} density < 0.248 pA/pF) was required to produce a stable pacemaking action potential with a 'valid' pacemaking frequency. With the increase of the I_{K1} inhibition level, the CL became shortened at all I_f densities considered. Also, the more that I_{K1} was inhibited, the less I_f was needed to provoke 'valid' spontaneous pacemaking activity. By contrast, the effect of I_f on the CL presented two phases, which was dependent on the I_{K1} density. When

287 I_{K1} was less than 0.198 pA/pF, the pacemaking ability became robust with the increase in I_f density. However, when I_{K1} was
288 increased from 0.198 to 0.248 pA/pF, an increase in I_f actually slowed the pacemaking activity, leading to an increased CL.

289 # Discussion

290 ## Summary of major findings

291 In this study, we construct a virtual bio-engineered pacemaking cell model based on a human VM model by a combination of
292 reduction of I_{K1} and incorporation of I_f. Using the developed bio-pacemaker model, we investigate the combined actions of
293 different I_{K1} and I_f permutations on the dynamical behaviours of membrane potential, ionic channel currents and intracellular ionic
294 concentrations. It is shown that robust and stable pacemaking activity can be established by balancing the actions of reduced I_{K1}
295 and increased I_f, though the effect of each manipulation on pacemaking activity is different. While the action of a reduced I_{K1} on
296 the pacemaking activity is consistent, that of an increased I_f is biphasic. Whilst the incorporation of I_f at an appropriate level
297 promotes pacemaking activity, excessive I_f might result in abnormal pacemaking activity accompanied by abnormal intracellular
298 ionic concentrations, which could be proarrhythmic. As a result, the reciprocal interaction between I_{K1} and I_f is crucial for
299 producing stable spontaneous pacemaking activity in VMs. The results of this study may be useful for optimizing the future
300 design of engineered bio-pacemakers.

301 ## Role of I_{K1} suppression on pacemaking activity

302 The suppression of I_{K1} plays an important role in the generation of pacemaking activities in the VM cell model. Our simulation
303 results have shown that a significant I_{K1} suppression (at least 60%) with the incorporation of I_f is required to provoke
304 auto-rhythmicity in the model. With a modest suppression (i.e. 60-75% suppression of I_{K1}), only unstable spontaneous APs can be
305 produced. When I_{K1} is further suppressed by 75% - 100%, persistent, steady pacemaking behaviour can be initiated in our model
306 with appropriate incorporation of I_f (Fig 4). These simulation results are in consistence with those of experimental findings, where
307 it has been found that I_{K1} could be suppressed by 50 – 90 % by knocking out the Kir2.1 gene, and more than 80% inhibition of I_{K1}

was required to produce a pacemaking phenomenon in guinea-pig's ventricular cavity (11, 20). It is also in agreement with previous bifurcation analyses in showing that it required I_{K1} to be reduced to at least 15% of the control value to transform a VM cell model to be auto-rhythmic (46). and a complete block of I_{K1} produced a spontaneous pacemaking activity with a CL of 795 ms (46), close to 833 ms when I_{K1} was totally suppressed in the present study. We have also found a monotonic relationship between the measured CL and the degree of I_{K1} suppression. It suggests that when I_{K1} is inhibited enough to induce automaticity, the more the I_{K1} is blocked, the faster the pacemaking activity is with all I_f densities considered (Fig 8). Similar results have also been observed in another ventricular cell model developed for human VMs (53) based on modifications of the model of O'Hara and Rudy (54) (S1 Text and S8 Fig, solid and dotted lines).

Though our simulation results suggest an important role of sufficient suppression of I_{K1} for generating persistent and stable pacemaking APs, it is noteworthy that the deficiency of I_{K1} has been reported to be lethal for adult rodents (55); and loss function of *Kir2* gene may prolong QT intervals as well as cause Andersen's syndrome (56). Consequently, suppression of I_{K1} from VM for generating a biological pacemaker may only be suitable when applied to highly localized, designated 'pacemaker' regions.

Role of I_f in pacemaking activity

I_f has been shown to play an important role in generating pacemaking APs in both native (13, 21, 27, 28, 35, 36) and engineered pacemakers (42). Experimentally it has been shown that high expression of *HCN2* can initiate spontaneous beats in neonatal rat VMs (21, 35) and improve spontaneous beats in rabbit CMs (13). *HCN4* incorporation by the expression of *TBX18* can also initiate spontaneous pacemaking activity in both rodent VMs (10) and porcine VMs (12).

In the present study, we have also highlighted the role of I_f in generating pacemaking activity. Our simulation results have shown that with different I_f densities, the pacemaking activity may present different behaviours, including transient automaticity with self-termination, bursting behaviour, and persistent pacemaking (Fig 4). The incorporation of low amplitude of I_f can help to boost the pacemaking activity in the VM-based pacemaker model induced by I_{K1}-inhibition (Fig 5). It helped to promote pacemaking

activity, *via* its action of depolarization during the diastolic depolarization phase as well as its action on the intracellular ion concentrations. It has been shown that the inclusion of I_f in the VM cell model causes the accumulation of $[Na^+]_i$, which enhances Na^+/Ca^{2+} exchange, thus promoting membrane potential depolarization especially during the early stage of DI (Fig 5). Such a promoting action of I_f in bio-pacemaking was also shown in another ventricular cell model as shown in S1 Text (S8 Fig, solid and dashed lines).

An increase in I_f density can enhance the automaticity in most cases. However, the effect of I_f on the pacemaking activity was observed to be biphasic. In our simulation, increasing I_f from a small initial density was associated with an increased pacemaking rate manifested by a decreased CL. But when it was increased to be over -2.52 pA/pF, excessive I_f resulted in an elevated MDP (Fig 6 B), which caused a reduced activation of I_f and I_{Na} (Fig 6 E and F), leading to a slowdown of the ability of pacemaking activity. The negative effect of excessive I_f on pacemaking APs was also observed in another ventricular pacemaker model (53) (S1 Text). A further increase in I_f density even terminated pacemaking activity (S9 Fig). This mechanism is verified by the fact that in the bio-pacemaker induced by HCN2 expression (57), co-expression of the skeletal muscle sodium channel 1 (*SkM1*), in order to hyperpolarize the action potential threshold, helped to counterbalance the negative effect of I_f overexpression, producing an accelerated depolarization phase. Furthermore, when I_{K1} was at a high value (e.g. density at 0.198 pA/pF), acute I_f even lengthened pacemaking period (Fig 7 A, black line). This simulation result is in agreement with a previous biological experimental study that observed a negative action of acute HCN gene expression in cardiac automaticity (41).

Reciprocal interaction between I_{K1} and I_f

Our study demonstrated that the reciprocal interaction between I_{K1} and I_f plays a crucial role in creating stable and persistent pacemaking. The present study has shown that only an optimal combination of I_{K1} and I_f can initiate stable pacemaking activity (Fig 4). In the presence of I_f, the greater the degree of I_{K1} suppression, the smaller was the I_f density required for the generation of spontaneous oscillation (Fig 4). And modulation of the two currents simultaneously helps to create a physiologically-like

pacemaker that is better than that produced by manipulating I_{K1} or I_f alone (Fig 8). Such observation of reciprocal interaction between I_{K1} and I_f in pacemaking is consistent with previous experimental observations. Previous studies have shown that although suppressing I_{K1} (11, 20), or incorporating sufficient I_f (21) alone was able to initiate pacemaking activity in VM cells, a pacemaker constructed by *TBX18* showed greater stability, due to its combined actions of I_{K1} reduction and I_f increase (10). Another experiment in porcine VMs (12) also indicated that *TBX18* expression did not increase the risk of arrhythmia, which means that a mixed-current approach is probably a superior means of producing a bio-pacemaker. Experiments in a *Kir2.1*/*HCN2* HEK293 cell (44) and *Kir2.1*/*HCN4* (42) showed that I_{K1} may actually recruit more I_f by activating current at more negative membrane voltages, because I_{K1} was the only negative current in these experiments. Our simulation, however, did not yield such a result because the interaction of other positive currents (such as I_{NaK}, I_{Kr} and I_{Ks}) contributed to the hyperpolarization of membrane potential and helped the activation of I_f.

In addition, simulation results showed that I_{K1} expression level may influence the I_f's effect on the pacemaking activity. Excessive I_{K1} hindered I_f's ability to modulate pacemaking activity (Fig 7A and Fig 8). An experiment showed a coincident result that the expression of HCN2 in adult rat VMs could not cause spontaneous beats due to the high expression of I_{K1} (21), but in neonatal rats, the I_{K1} was less so that expressing HCN2 could provoke automaticity.

Limitations

The limitations of human VMs model we used in this study has been described elsewhere (58). In this study, the I_f formulation of human SAN (51) was incorporated into the original VMs model. The properties of I_f, including the conductance of I_f, the half-maximal activation voltage ($V_{1/2}$) and time constants of the activation, may present species-dependence. In this study, we only consider the conductance of I_f but have not discussed other properties of I_f.

In addition, in this study, we only investigated the pacemaking action potential at the single-cell level, without considering the intercellular electrical coupling between pacemaker cells as presented in the SAN tissue. Mathematical analysis showed that the

incorporation of I_{st} and I_{CaT} into VMs may promote the pacemaking ability of ventricular pacemaker in the coupled-cell model (49). However, up to now, there is no experimental study conducted yet to produce pacemaker cells from VMs by modifying the expression of I_{st} and I_{CaT}, thus we did not discuss them in the present study. It is necessary to highlight these limitations, they nevertheless do not affect our conclusions on the underlying pacemaking mechanisms of engineered bio-pacemaker cells, especially regarding the reciprocal interaction of I_{K1} and I_f for a robust bio-pacemaker in modified VMs.

Methods

Single bio-pacemaker cell model

Previous experimental studies (10, 11, 19-21) implemented the suppression of *Kir2.1*, the incorporation of *HCN* channels and the expression of *TBX18* to induce pacemaking in VMs. In this study, we used a mathematical model of human VMs (50) as the basal model to investigate possible pacemaking mechanisms in VM-transformed pacemaking cells. In brief, the basal VM cell model can be described by the following ordinary differential equation:

$$\frac{dV}{dt} = -\frac{I_{ion}}{C_m} \quad (1)$$

where V is the voltage across cell membrane surfaces, t is time, I_{ion} is the sum of all transmembrane ionic currents, and C_m cell capacitance.

The I_{ion} in the original ventricular model is described by the following equation:

$$I_{ion} = I_{Na} + I_{K1} + I_{to} + I_{Kr} + I_{Ks} + I_{CaL} + I_{NaCa} + I_{NaK} + I_{pCa} + I_{pK} + I_{bCa} + I_{bNa} \quad (2)$$

where I_{Na} is fast sodium channel current, I_{K1} is inward rectifier potassium channel current, I_{to} is transient outward current, I_{Kr} is rapid delayed rectifier potassium channel current, I_{Ks} is slow delayed rectifier potassium channel current, I_{NaCa} is Na^+/Ca^{2+} exchange current, I_{NaK} is Na^+/K^+ pump current, I_{pCa} and I_{pK} are plateau Ca^{2+} and K^+ currents, and I_{bCa} and I_{bNa} are background Ca^{2+} and Na^+ currents. The formulations and their parameters for the ionic channels of human VM cells were listed in Ref. (50, 58).

To mimic the reduction of *Kir2.1* expression (11, 19, 20) or suppressing I_{K1} by expressing *TBX18* (10), in simulations, I_{K1} was decreased by modulating its macroscopic channel conductance (G_{K1}). To mimic the incorporation of I_f in VMs experimentally (21), we modified the basal model of Eq. 2 by incorporating human SAN I_f formulation (51). In simulations, I_f was modulated by changing its channel conductance (G_f).

As a result, the I_{ion} for the bio-pacemaker model can be described as:

$$I_{ion} = I_{Na} + I_{K1} + I_{to} + I_{Kr} + I_{Ks} + I_{CaL} + I_{NaCa} + I_{NaK} + I_{pCa} + I_{pK} + I_{bCa} + I_{bNa} + I_f \quad (3)$$

where I_{K1} could be expressed by

$$I_{K1} = S_{K1}\, G_{K1} \sqrt{\frac{K_o}{5.4}}\, x_{k1\infty}\, (V_m - E_k) \quad (4)$$

where G_{K1} is the conductance of I_{K1}, $x_{k1\infty}$ is a time-independent inward rectification factor, K_o is extracellular K^+ concentration and E_K is the equilibrium potentials of K^+. S_{K1} is a scaling factor used to simulate the change of I_{K1} expression level.

I_f has two ionic channels and could permeate Na^+ and K^+ respectively. I_f could be described by

$$I_f = I_{f,Na} + I_{f,K} \quad (5)$$

$$I_{f,Na} = S_f\, G_{f,Na}\, y\, (V - E_{Na}) \quad (6)$$

$$I_{f,K} = S_f\, G_{f,K}\, y\, (V - E_K) \quad (7)$$

where $G_{f,Na}$ and $G_{f,K}$ are maximal $I_{f,Na}$ and $I_{f,K}$ channel conductance, y is a time-independent inward rectification factor that is a function of voltage, E_{Na}, E_K are equilibrium potentials of Na^+ and K^+ channels respectively, and S_f is a scaling factor used to simulate the change of I_f expression level.

Formulations of other channel currents for the VM cell model are the same as those in the original model in Ref. (50).

Evaluating criterion of the pacemaking stability and ability

To analyse the effect of I_{K1} and I_f on pacemaking activity, we simulated the membrane potential under different current densities of I_{K1} and I_f, with I_{K1} being reduced systematically by from 60% to 100% (i.e., I_{K1} density at -80 mV changed from 0.396 to 0 pA/pF while the I_{K1} density in the original basal model is 0.99 pA/pF at -80 mV in I-V curve). The representative I-V relation curve under different inhibition of I_{K1} is shown in S1A Fig. I_f density was increased by from 0 to 10 folds with a basal value of -0.63 pA/pF at -80 mV in I-V curve (i.e., I_f density changed from 0 to -6.3 pA/pF at -80 mV). The representative I-V relation curve under different incorporation of I_f is shown in S1B Fig.

Two characteristics were used to quantify the state of membrane potentials generated by the ventricular pacemaker model: the continuity and validity of spontaneous APs. The continuity was used to quantify whether or not the automaticity of membrane potential could sustain with time; whilst the validity was used to characterize whether every automatic wave was biologically-valid or not. As such, we defined the following:

W: a valid wave. An action potential whose wave trough was less than -20 mV and wave crest was more than 20 mV could be considered as a valid wave.

αW, $\alpha<1$: an incomplete wave.

R: a resting period lasting 1000 ms.

W^n: the concatenation of n W's.

(W R): the concatenation of W and R.

As such, none pacemaking behaviour during the entire simulation period could be described as State-1:

$$R^n,\ n \in N^+ \tag{8}$$

Transient spontaneous pacemaking behaviour could be described as State-2:

$$(W^m, R^n),\ m, n \in N^+ \tag{9}$$

Bursting pacemaking behaviour could be described as State-3:

$$(W^{mi}, R^{ni})^M,\ i \in [1,M],\ M, m_i, n_i \in N^+ \tag{10}$$

Persistent pacemaking activity with periodically incomplete depolarization could be described as State-4:

$$(W^m, \alpha W)^M,\ \alpha<1,\ m, M \in N^+ \tag{11}$$

Stable pacemaking activity could be described as State-5:

$$W^m,\ m \in N^+ \tag{12}$$

With regard to the pacemaking ability, when the pacemaking behaviour was stable, the cycle length (CL) under varied I_{K1} and I_f was calculated. The CL was defined as the averaged wavelength of pacemaking activity over a period of simulation of over 4×10^5 ms, ensuring the accuracy of the computed CL. As the basal model was for VMs, a long simulation period was necessitated to achieve a completely stable pacemaking status and minimize the effect of the transition period.

Characteristics of pacemaking during diastolic interval

The length of the diastolic interval (DI) is an important measure to characterize the pacemaking ability. In this study, we defined that DI as the time interval between the time of maximum diastolic potential (MDP) (S6A Fig, t_1) and the time when the membrane potential reaches at -55 mV (i.e., around the activation potential of the I_{CaL}) (S6A Fig, t_2). The diastolic upstroke velocity during DI was defined as the change rate of the membrane potential, taking the following formulation:

$$\text{diastolic upstroke velocity} = \frac{\text{MDP} - (-55)}{t_2 - t_1} \tag{13}$$

The unit of diastolic upstroke velocity was V/s.

The main inward currents which helped to depolarize membrane potential during DI are I_{Na}, I_{NaCa} and I_f. Their contribution can be described by an average integral during DI:

$$I_{in} = \frac{\int_{t_1}^{t_2}(I_{Na} + I_{NaCa} + I_f)}{t_2 - t_1} \quad (14)$$

Similarly, the main outward currents which held membrane potential at diastolic potential during DI are I_{K1}, I_{NaK}, I_{Kr} and I_{Ks}, the integral of which can be described as:

$$I_{out} = \frac{\int_{t_1}^{t_2}(I_{K1} + I_{NaK})}{t_2 - t_1} \quad (15)$$

Supporting Information

S1 Fig. The I-V curve of I_{K1} and I_f with different expression level.

S_{K1} and S_f are defined as scaling factors used to simulate the change of I_{K1} and I_f expression level. (A) The I-V curve of I_{K1} with S_{K1} of 1, 0.4, 0.1 that gives I_{K1} densities in the I-V curve at -80 mV 0.99, 0.396 and 0.099 pA/pF respectively. (B) The I-V curve of I_f with S_f of 1, 5, 10 that gives I_f densities in the I-V curve at -80 mV -0.63, -3.15 and -6.3 pA/pF respectively.

S2 Fig. Na^+/Ca^{2+} exchange current (I_{NaCa}) of a transient pacemaking behaviour.

(A) I_{NaCa} during the entire simulating period of 800 s with the current densities of (I_{K1}, I_f) at (0.297pA/pF, -1.89 pA/pF). (B) Expanded plots of I_{NaCa} traces for the time course from 1.6×10^5 to 1.64×10^5 ms marked by the horizontal brackets with asterisks in (A).

S3 Fig. Transient spontaneous pacemaking behaviour.

Membrane potential (V) during the entire simulation period of 400 s with the current densities of (I_{K1}, I_f) at (0.178 pA/pF, -0.63 pA/pF).

S4 Fig. Na^+/Ca^{2+} exchange current (I_{NaCa}) of a bursting pacemaking behaviour.

(A) I_{NaCa} with the current densities of (I_{K1}, I_f) at (0.297 pA/pF, -2.52 pA/pF) during the entire simulating period of 800 s. (B) Expanded plots of I_{NaCa} traces for the time course from 3.83×10^5 ms to 3.85×10^5 ms marked by the horizontal brackets with asterisks in (A).

S5 Fig. Partial failure of spontaneous action potentials with different densities of I_{K1}.

(A) Membrane potential (V) with the current densities of (I_{K1}, I_f) at (0.297 pA/pF, -3.15 pA/pF) during simulating time course from 3.6×10^5 to 3.7×10^5 ms. (B) Membrane potential (V) with the current densities of (I_{K1}, I_f) at (0.277 pA/pF, -3.15 pA/pF) during simulating time course from 3.6×10^5 to 3.7×10^5 ms.

S6 Fig. Change of diastolic depolarizing rate with the increase of I_f density.

(A) Definition of diastolic depolarizing rate. MDP: maximum diastolic potential; t_1: the time when membrane potential is MDP; t_2: the time when potential arrives -55 mV (i.e., around the activation potential of the I_{CaL}). (B) Change of diastolic depolarizing rate with the increase of I_f density from 0 to -6.3 pA/pF when I_{K1} density at -80 mV is at 0.05 pA/pF.

S7 Fig. Prolonged cycle length under greater I_f density.

Membrane potential (V) with the current densities of (I_{K1}, I_f) at (0.05 pA/pF, -3.78 pA/pF) and (0.05 pA/pF, -5.04 pA/pF) (solid and dotted line respectively).

S8 Fig. Model-dependence test – stable pacemaking behaviour.

Membrane potential (V) with the current densities of (I_{K1}, I_f) at (0.198 pA/pF, -0.63 pA/pF), (0.178 pA/pF, -0.63 pA/pF) and (0.198 pA/pF, -0.756 pA/pF) (solid, dotted and dashed line respectively) based on a human ventricular myocytes model.

S9 Fig. Model-dependence test – failed pacemaking activity.

Membrane potential (V) with the current densities of (I_{K1}, I_f) at (0.198 pA/pF, -1.26 pA/pF) based on a human ventricular myocytes model.

S1 Text. Model-dependence test.

Author Contributions

Conceptualization: Henggui Zhang.

Data curation: Yacong Li.

Formal analysis: Yacong Li, Henggui Zhang, Jules C. Hancox.

Funding acquisition: Henggui Zhang.

Investigation: Yacong Li.

Methodology: Yacong Li, Qince Li, Henggui Zhang.

Project administration: Kuanquan Wang, Henggui Zhang.

Resources: Kuanquan Wang, Henggui Zhang.

Software: Yacong Li, Henggui Zhang.

Supervision: Kuanquan Wang, Henggui Zhang.

Validation: Yacong Li.

Visualization: Yacong Li, Henggui Zhang.

Writing – original draft: Yacong Li.

Writing – review & editing: Henggui Zhang, Jules C. Hancox.

References

1. Cohen IS, Brink PR, Robinson RB, Rosen MR. The why, what, how and when of biological pacemakers. Nat Clin Pract Card. 2005;2(8):374-5.

2. Rosen MR. Gene Therapy and Biological Pacing. New Engl J Med. 2014;371(12):1158-9.

3. Rosen MR, Brink PR, Cohen IS, Robinson RB. Cardiac pacing: from biological to electronic ... to biological? Circ Arrhythm Electrophysiol. 2008;1(1):54-61.

4. Rosen MR, Robinson RB, Brink PR, Cohen IS. The road to biological pacing. Nature reviews Cardiology. 2011;8(11):656-66.

5. Wilders R, Verheijck EE, Kumar R, Goolsby WN, van Ginneken AC, Joyner RW, et al. Model clamp and its application to synchronization of rabbit sinoatrial node cells. Am J Physiol. 1996;271(5 Pt 2):H2168-82.

6. Kapoor N, Galang G, Marban E, Cho HC. Transcriptional suppression of connexin43 by TBX18 undermines cell-cell electrical coupling in postnatal cardiomyocytes. J Biol Chem. 2011;286(16):14073-9.

7. Freudenberger RS, Wilson AC, Lawrence-Nelson J, Hare JM, Kostis JB. Permanent pacing is a risk factor for the development of heart failure. American Journal of Cardiology. 2005;95(5):671-4.

8. Cingolani E, Goldhaber JI, Marban E. Next-generation pacemakers: from small devices to biological pacemakers. Nature reviews Cardiology. 2018;15(3):139-50.

9. Shlapakova IN, Nearing BD, Lau DH, Boink GJJ, Danilo P, Kryukova Y, et al. Biological pacemakers in canines exhibit positive chronotropic response to emotional arousal. Heart Rhythm. 2010;7(12):1835-40.

10. Kapoor N, Liang WB, Marban E, Cho HC. Direct conversion of quiescent cardiomyocytes to pacemaker cells by expression of Tbx18. Nat Biotechnol. 2013;31(1):54-+.

11. Miake J, Marban E, Nuss HB. Functional role of inward rectifier current in heart probed by Kir2.1 overexpression and dominant-negative suppression. J Clin Invest. 2003;111(10):1529-36.

12. Hu YF, Dawkins JF, Cho HC, Marban E, Cingolani E. Biological pacemaker created by minimally invasive somatic reprogramming in pigs with complete heart block. Sci Transl Med. 2014;6(245).

13. Zhou YF, Yang XJ, Li HX, Han LH, Jiang WP. Mesenchymal stem cells transfected with HCN2 genes by LentiV can be modified to be cardiac pacemaker cells. Med Hypotheses. 2007;69(5):1093-7.

14. Gorabi AM, Hajighasemi S, Tafti HA, Atashi A, Soleimani M, Aghdami N, et al. TBX18 transcription factor overexpression in human-induced pluripotent stem cells increases their differentiation into pacemaker-like cells. Journal of cellular physiology. 2019;234(2):1534-46.

15. Noble D. The surprising heart: a review of recent progress in cardiac electrophysiology. The Journal of physiology. 1984;353:1-50.

16. DiFrancesco D. The contribution of the 'pacemaker' current (if) to generation of spontaneous activity in rabbit sino-atrial node myocytes. The Journal of physiology. 1991;434:23-40.

17. Mesirca P, Torrente AG, Mangoni ME. T-type channels in the sino-atrial and atrioventricular pacemaker mechanism. Pflugers Arch. 2014;466(4):791-9.

18. Guo J, Ono K, Noma A. A sustained inward current activated at the diastolic potential range in rabbit sino-atrial node cells. The Journal of physiology. 1995;483 (Pt 1):1-13.

19. Zaritsky JJ, Redell JB, Tempel BL, Schwarz TL. The consequences of disrupting cardiac inwardly rectifying K+ current (I-K1) as revealed by the targeted deletion of the murine Kir2.1 and Kir2.2 genes. J Physiol-London. 2001;533(3):697-710.

20. Miake J, Marban E, Nuss HB. Gene therapy - Biological pacemaker created by gene transfer. Nature. 2002;419(6903):132-3.

21. Qu JH, Barbuti A, Protas L, Santoro B, Cohen IS, Robinson RB. HCN2 overexpression in newborn and adult ventricular myocytes - Distinct effects on gating and excitability. Circ Res. 2001;89(1):E8-E14.

22. Qu JH, Plotnikov AN, Danilo P, Shlapakova I, Cohen IS, Robinson RB, et al. Expression and function of a biological pacemaker in canine heart. Circulation. 2003;107(8):1106-9.

23. Plotnikov AN, Sosunov EA, Qu JH, Shlapakova IN, Anyukhovsky EP, Liu LL, et al. Biological pacemaker implanted in canine left bundle branch provides ventricular escape rhythms that have physiologically acceptable rates. Circulation. 2004;109(4):506-12.

24. Ionta V, Liang WB, Kim EH, Rafie R, Giacomello A, Marban E, et al. SHOX2 Overexpression Favors Differentiation of Embryonic Stem Cells into Cardiac Pacemaker Cells, Improving Biological Pacing Ability. Stem Cell Rep. 2015;4(1):129-42.

25. Xue T, Cho HC, Akar FG, Tsang SY, Jones SP, Marban E, et al. Functional integration of electrically active cardiac derivatives from genetically engineered human embryonic stem cells with quiescent recipient ventricular cardiomyocytes - Insights into the development of cell-based pacemakers. Circulation. 2005;111(1):11-20.

26. Kehat I, Khimovich L, Caspi O, Gepstein A, Shofti R, Arbel G, et al. Electromechanical integration of cardiomyocytes derived from human embryonic stem cells. Nat Biotechnol. 2004;22(10):1282-9.

27. Bruzauskaite I, Bironaite D, Bagdonas E, Skeberdis VA, Denkovskij J, Tamulevicius T, et al. Relevance of HCN2-expressing human mesenchymal stem cells for the generation of biological pacemakers. Stem Cell Res Ther. 2016;7.

28. Zhang H, Li SC, Qu D, Li BL, He B, Wang C, et al. Autologous biological pacing function with adrenergic-responsiveness in porcine of complete heart block. Int J Cardiol. 2013;168(4):3747-51.

29. Planat-Benard V, Menard C, Andre M, Puceat M, Perez A, Garcia-Verdugo JM, et al. Spontaneous cardiomyocyte differentiation from adipose tissue stroma cells. Circ Res. 2004;94(2):223-9.

30. Choi YS, Dusting GJ, Stubbs S, Arunothayaraj S, Han XL, Collas P, et al. Differentiation of human adipose-derived stem cells into beating cardiomyocytes. J Cell Mol Med. 2010;14(4):878-89.

31. Chen L, Deng ZJ, Zhou JS, Ji RJ, Zhang X, Zhang CS, et al. Tbx18-dependent differentiation of brown adipose tissue-derived stem cells toward cardiac pacemaker cells. Mol Cell Biochem. 2017;433(1-2):61-77.

32. Chauveau S, Anyukhovsky EP, Ben-Ari M, Naor S, Jiang YP, Danilo P, et al. Induced Pluripotent Stem Cell-Derived Cardiomyocytes Provide In Vivo Biological Pacemaker Function. Circ-Arrhythmia Elec. 2017;10(5).

33. Gorabi AM, Hajighasemi S, Khori V, Soleimani M, Rajaei M, Rabbani S, et al. Functional biological pacemaker generation by T-Box18 protein expression via stem cell and viral delivery approaches in a murine model of complete heart block. Pharmacological research. 2019;141:443-50.

34. Kleber AG, Rudy Y. Basic mechanisms of cardiac impulse propagation and associated arrhythmias. Physiol Rev. 2004;84(2):431-88.

35. Potapova I, Plotnikov A, Lu ZJ, Danilo P, Valiunas V, Qu JH, et al. Human mesenchymal stem cells as a gene delivery system to create cardiac pacemakers. Circ Res. 2004;94(7):952-9.

36. Plotnikov AN, Shlapakova I, Szabolcs MJ, Danilo P, Lorell BH, Potapova IA, et al. Xenografted adult human mesenchymal stem cells provide a platform for sustained biological pacemaker function in canine heart. Circulation. 2007;116(7):706-13.

37. Saito Y, Nakamura K, Yoshida M, Sugiyama H, Ohe T, Kurokawa J, et al. Enhancement of Spontaneous Activity by HCN4 Overexpression in Mouse Embryonic Stem Cell-Derived Cardiomyocytes - A Possible Biological Pacemaker. Plos One. 2015;10(9).

38. Cho HC, Kashiwakura Y, Marban E. Creation of a biological pacemaker by cell fusion. Circ Res. 2007;100(8):1112-5.

39. Azene EM, Xue T, Marban E, Tomaselli GF, Li RA. Non-equilibrium behavior of HCN channels: Insights into the role of HCN channels in native and engineered pacemakers. Cardiovasc Res. 2005;67(2):263-73.

40. Lieu DK, Chan YC, Lau CP, Tse HF, Siu CW, Li RA. Overexpression of HCN-encoded pacemaker current silences bioartificial pacemakers. Heart Rhythm. 2008;5(9):1310-7.

41. Kuwabara Y, Kuwahara K, Takano M, Kinoshita H, Arai Y, Yasuno S, et al. Increased Expression of HCN Channels in the Ventricular Myocardium Contributes to Enhanced Arrhythmicity in Mouse Failing Hearts. J Am Heart Assoc. 2013;2(3).

42. Sun Y, Timofeyev V, Dennis A, Bektik E, Wan XP, Laurita KR, et al. A Singular Role of I-K1 Promoting the Development of Cardiac Automaticity during Cardiomyocyte Differentiation by I-K1-Induced Activation of Pacemaker Current. Stem Cell Rev Rep. 2017;13(5):631-43.

43. Yang M, Zhang GG, Wang T, Wang X, Tang YH, Huang H, et al. TBX18 gene induces adipose-derived stem cells to differentiate into pacemaker-like cells in the myocardial microenvironment. Int J Mol Med. 2016;38(5):1403-10.

44. Chen K, Zuo D, Wang SY, Chen H. Kir2 inward rectification-controlled precise and dynamic balances between Kir2 and HCN currents initiate pacemaking activity. FASEB J. 2018;32(6):3047-57.

45. Silva J, Rudy Y. Mechanism of pacemaking in I-K1-downregulated myocytes. Circ Res. 2003;92(3):261-3.

46. Kurata Y, Hisatome I, Matsuda H, Shibamoto T. Dynamical mechanisms of pacemaker generation in I-K1-downregulated human ventricular myocytes: Insights from bifurcation analyses of a mathematical model. Biophys J. 2005;89(4):2865-87.

47. Tong WC, Holden AV. Induced pacemaker activity in virtual mammalian ventricular cells. Lect Notes Comput Sc. 2005;3504:226-35.

48. Kurata Y, Matsuda H, Hisatome I, Shibamoto T. Roles of hyperpolarization-activated current If in sinoatrial node pacemaking: insights from bifurcation analysis of mathematical models. American journal of physiology Heart and circulatory physiology. 2010;298(6):H1748-60.

49. Kurata Y, Matsuda H, Hisatome I, Shibamoto T. Effects of pacemaker currents on creation and modulation of human ventricular pacemaker: theoretical study with application to biological pacemaker engineering. American journal of physiology Heart and circulatory physiology. 2007;292(1):H701-18.

50. ten Tusscher KH, Panfilov AV. Alternans and spiral breakup in a human ventricular tissue model. American journal of physiology Heart and circulatory physiology. 2006;291(3):H1088-100.

51. Fabbri A, Fantini M, Wilders R, Severi S. Computational analysis of the human sinus node action potential: model development and effects of mutations. The Journal of physiology. 2017;595(7):2365-96.

52. Verkerk AO, Wilders R, van Borren MM, Peters RJ, Broekhuis E, Lam K, et al. Pacemaker current (I(f)) in the human sinoatrial node. Eur Heart J. 2007;28(20):2472-8.

53. Whittaker DG, Ni H, Benson AP, Hancox JC, Zhang H. Computational Analysis of the Mode of Action of Disopyramide and Quinidine on hERG-Linked Short QT Syndrome in Human Ventricles. Frontiers in physiology. 2017;8:759.

615 54. O'Hara T, Virag L, Varro A, Rudy Y. Simulation of the undiseased human cardiac ventricular action potential: model
616 formulation and experimental validation. PLoS computational biology. 2011;7(5):e1002061.

617 55. Irnich W, de Bakker JM, Bisping HJ. Electromagnetic interference in implantable pacemakers. Pacing Clin Electrophysiol.
618 1978;1(1):52-61.

619 56. Plaster NM, Tawil R, Tristani-Firouzi M, Canun S, Bendahhou S, Tsunoda A, et al. Mutations in Kir2.1 cause the
620 developmental and episodic electrical phenotypes of Andersen's syndrome. Cell. 2001;105(4):511-9.

621 57. Boink GJJ, Duan L, Nearing BD, Shlapakova IN, Sosunov EA, Anyukhovsky EP, et al. HCN2/SkM1 Gene Transfer Into
622 Canine Left Bundle Branch Induces Stable, Autonomically Responsive Biological Pacing at Physiological Heart Rates. J Am Coll
623 Cardiol. 2013;61(11):1192-201.

624 58. ten Tusscher KHWJ, Noble D, Noble PJ, Panfilov AV. A model for human ventricular tissue. Am J Physiol-Heart C.
625 2004;286(4):H1573-H89.

626